[9] a) H. Bevsek, M. Ahmed, D. S. Peterka, F. C. Sailes, A. G. Suits, *Faraday Discuss.* **1998**, *108*, 131; b) M. Ahmed, D. A. Blunt, D. Chen, A. G. Suits, *J. Chem. Phys.* **1997**, *106*, 7617.
[10] a) D. S. Peterka, M. Ahmed, A. G. Suits, K. J. Wilson, A. Korkin, M. Nooijen, R. J. Bartlett, *J. Chem. Phys.* **1999**, *110*, 6095; b) D. S. Peterka, M. Ahmed, A. G. Suits, K. J. Wilson, A. Korkin, M. Nooijen, R. J. Bartlett, *J. Chem. Phys.* **1999**, *111*, 5279 (erratum).
[11] a) G. I. Gellene, R. F. Porter, *Acc. Chem. Res.* **1983**, *16*, 200; b) C. Wesdemiotis, F. W. McLafferty, *Chem. Rev.* **1987**, *87*, 485; c) J. L. Holmes, *Mass Spectrom. Rev.* **1989**, *24*, 620; d) F. W. McLafferty, *Science* **1990**, *247*, 925; e) N. Goldberg, H. Schwarz, *Acc. Chem. Res.* **1994**, *27*, 347; f) D. V. Zagorevskii, J. L. Holmes, *Mass Spectrom. Rev.* **1994**, *13*, 133; g) C. A. Schalley, G. Hornung, D. Schröder, H. Schwarz, *Chem. Soc. Rev.* **1998**, *27*, 91.
[12] F. Cacace, G. de Petris, F. Pepi, A. Troiani, *Science* **1999**, *285*, 81.
[13] F. Cacace, G. de Petris, F. Pepi, A. Troiani, *Angew. Chem.* **2000**, *112*, 375; *Angew. Chem. Int. Ed.* **2000**, *39*, 367.
[14] K. S. Griffith, G. I. Gellene, *J. Chem. Phys.* **1992**, *96*, 4403, and references therein.
[15] The minor $^{16}O^{18}O^+$ fragment with $m/z = 34$ displayed by the CAD and the NR spectra is traced to the contribution from $^{16}O^{18}O$ present in the $^{18}O_2$ sample utilized, and from undissociated, doubly charged $^{16}O_2{}^{18}O_2{}^{2+}$ ions.
[16] R. D. Cohen, C. D. Sherrill, *J. Chem. Phys.* **2001**, *114*, 8257.
[17] a) W. E. Thompson, M. E. Jacox, *J. Chem. Phys.* **1989**, *91*, 3826; b) L. B. Knight, S. T. Cobranchi, J. Petty, *J. Chem. Phys.* **1989**, *91*, 4426.
[18] a) D. C. Conway, *J. Chem. Phys* **1969**, *50*, 3864; b) J. B. Peel, *J. Chem. Phys.* **1991**, *94*, 5774; c) J. B. Peel, *Chem. Phys. Lett.* **1994**, *218*, 367.
[19] a) R. Lindh, L. A. Barnes, *J. Chem. Phys.* **1994**, *100*, 224; b) L. A. Barnes, R. Lindh, *Chem. Phys. Lett.* **1994**, *223*, 207.
[20] M. E. Jacox, W. E. Thompson, *J. Chem. Phys.* **1994**, *100*, 750.
[21] K. Hiraoka, *J. Chem. Phys.* **1988**, *89*, 3190.
[22] F. A. Gorelli, L. Ulivi, M. Santoro, R. Bini, *Phys. Rev. Lett.* **1999**, *83*, 4093.
[23] F. A. Gorelli, L. Ulivi, M. Santoro, R. Bini, *Phys. Rev. B* **2001**, *63*(10), article 104110.

Fundamental Zeolite Crystal Growth Rates from Simulation of Atomic Force Micrographs**

Jonathan R. Agger,* Noreen Hanif, and Michael W. Anderson*

Insight into zeolite crystal growth is afforded by a computer model that simulates atomic force microscopy (AFM) images[1] of zeolite A crystallite surfaces. This leads to the first ever quantification of fundamental zeolite crystal growth processes. AFM enables imaging of nonconducting surfaces with atomic-scale vertical resolution and is ideal for probing the surface of inorganic crystals. The first AFM image of a zeolite, which depicted the cleaved (100) face of clinoptilolite, was published by Weisenhorn et al. in 1990.[2] This triggered a series of mineral zeolite studies[3] that used extremely detailed topographical information obtained from AFM images to estimate unit cell parameters. At lower resolution the imaging of atomic corrugations is precluded; however, there still remains a great wealth of information to be garnered concerning crystal growth processes.

Zeolite growth often occurs by the deposition of successive layers thus creating surface terraces.[1] Typically, terrace height, orientation, and shape are governed by the unit-cell structure and symmetry of the zeolite. Terrace separation usually decreases towards the extremity of the growing face, thus generating an overall parabolic cross-section. This quadratic relationship implies that it is terrace area and not size that grows at constant rate.[1b] Constant-area-deposition growth therefore predominates and this has significant ramifications on the mode of transport of gel nutrient to the growing face, as will be discussed later. As an introduction, an overview is given of specific features observed on the surface of zeolite A, chosen owing to its paramount industrial importance, cubic symmetry (facilitating creation of the model), and the existence of high-quality AFM images of its surface.

Atomic force micrographs of the (100) face of zeolite A crystallites reveal square-shaped surface terraces of uniform height equal to 1.2 nm, that is half the unit-cell dimension (Figure 1; squares are distorted to parallelograms owing to crystal tilt). The terrace edges run parallel to the edges of the crystal face. A further feature is that of curved terrace edges that have been postulated to arise during the coalescence of individual nucleation centers.[1b] The shape and surface density of these terraces are a result of the crystal growth mechanism. This work is concerned with simulation of such AFM images using the rates of fundamental crystal growth processes as variables in the model.

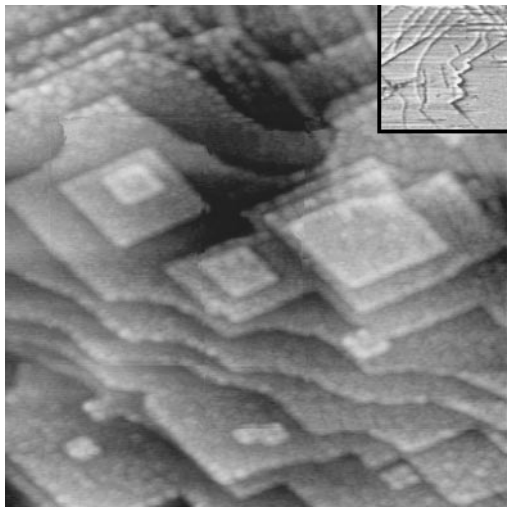

Figure 1. $1.0 \times 1.0\ \mu m^2$ AFM Tapping Mode image of a portion of a $10.0 \times 10.0\ \mu m^2$ (100) face of a zeolite A crystallite. Inset: phase image showing a section with a convex terrace growth front.

These AFM observations serve both as a basis for creation of the computer code and also provide a means of testing the

[*] Dr. J. R. Agger, Prof. M. W. Anderson, Dr. N. Hanif
UMIST Centre for Microporous Materials
PO Box 88, Manchester, M60 1QD (UK)
Fax: (+44) 161-200-4559
E-mail: j.agger@umist.ac.uk
m.anderson@umist.ac.uk

[**] J.R.A. gratefully acknowledges the EPSRC for Advanced Fellowship no AF/990985 and N.H. acknowledges financial support from the EPSRC.

  1433-7851/01/4021-4065 $ 17.50+.50/0

accuracy of different models. Herein we reveal the relative rates of individual crystal-growth processes in a zeolite for the first time, and thus make an important step towards understanding the crystallization of an extremely important class of open-framework inorganic materials.

The purpose of this study is to determine relative growth rates of surface terraces. It is not the purpose to determine the precise units of attachment at the face of a growing crystallite. The very existence of terraces implies stable surface terminations (possibly closed cages—but this is as yet undetermined). These surface structures can be achieved by addition of monomeric silica or alumina or oligomeric units. We concern ourselves only with the nature of the point of attachment.

Owing to the cubic symmetry of zeolite A, a two-dimensional grid may be employed to represent the (100) growing face—this study employed a 100 by 100 grid. During the simulation, the evolution in height of each position on the surface is measured in terms of the number of growth layers—each layer has been shown to comprise a beta cage and a double four-ring (D4R)—although the exact manner of surface termination remains as of yet unclear. The nature of the surface at a given position is defined by the relative presence of vicinal growth terraces. It is thus possible to define five sites, named arbitrarily. Initially, all sites on the surface are termed SURFACE sites, see Figure 2a. There are no vicinal terraces and any deposition must involve nucleation. The presence of one vicinal terrace is typical of sites found along the edge of an advancing terrace front. These sites, depicted in Figure 2b, are termed EDGE sites. A kink in a terrace front or a coalescence of two orthogonal terrace fronts will create a site, which has two vicinal terraces. These sites, depicted in Figure 2c, are termed KINK sites. The final two sites, depicted in Figure 2d and e, have three and four vicinal terraces and are termed U site and SURROUND site, respectively.

This simple representation of the (100) face as a grid and the definition of various types of surface site form the basis of the model used. It is noteworthy that such sites, for an open-framework material, are more complex than the usual definition for a dense-phase material where a neighboring site is usually an individual atom. Deposition of nutrient at the surface is simulated by incrementing the height variable of a given position on the surface and altering site geometries in the vicinity accordingly. Thus far the model is both idealogically trivial and easily programmed. Complexity arises from consideration of the method for allocating surface growth positions due to the inherent need for this process to be justified in a real physical sense.

The program works by defining growth times for the different site types—specific values will be discussed later. Every iteration, the program checks for growth at the different site types in the sequential order SURFACE, EDGE, KINK, U (in the final version of the code it was found to be unnecessary to differentiate between U and SURROUND sites). If no site type is destined for growth then the counter is incremented until a site type is primed. Once a type has been selected then one such site is chosen at random. After incrementing the surface height at that point by one unit, adjacent site geometries are recalculated and the iteration is repeated.

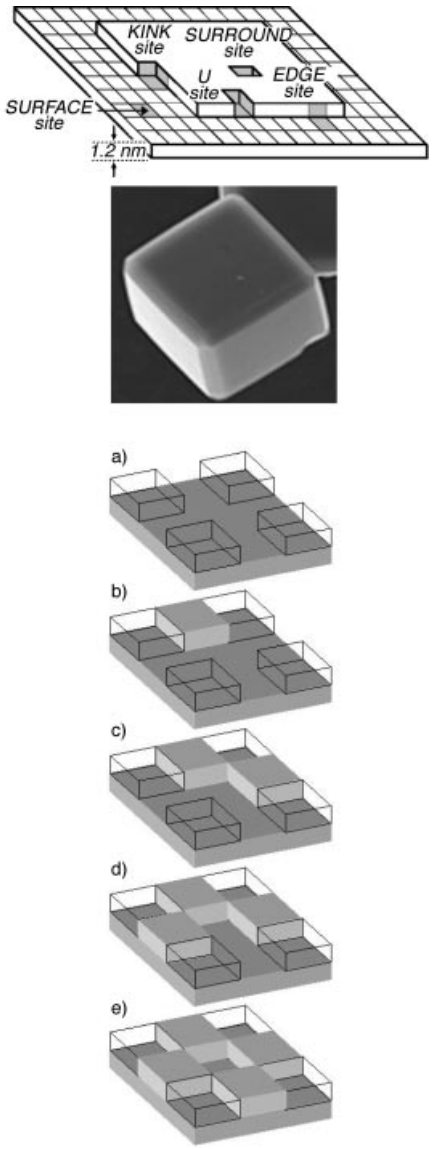

Figure 2. Scanning electron microscopy (SEM) image of the (100) face of a $10.0 \times 10.0 \times 10.0\ \mu m^3$ zeolite A crystallite (center), the five possible sites considered in modeling the growth process (a–e), and a schematic of a typical surface arrangement (top). The five sites are termed: a) SURFACE site, b) EDGE site, c) KINK site, d) U site, and e) SURROUND site, with zero, one, two, three, and four adjacent growth units, respectively. In each case, the potential growth site is located in the center of the upper layer. Diagonally adjacent surface units do not influence site definition in this current model and are hence shown as wire frames.

Transport of gel nutrient may now be considered. Diffusion-limited growth implies intermittent supply of nutrient to the crystal surface and is strongly influenced by population distribution of site types, as well as energetics of attachment. Thus growth is more probable at a large square-shaped terrace with many EDGE sites than at a small square-shaped terrace with fewer EDGE sites. Such growth, characterized by constant linear terrace advance, is refuted by experimental evidence, in images recorded on zeolites A, Y, and silicalite. These images are recorded on crystallites removed from gels at the end of synthesis, thus growth is not diffusion-limited

  1433-7851/01/4021-4066 $ 17.50+.50/0

even when supersaturation levels of aluminate and silicate are low. This is in contrast to template transport which has been shown to be diffusion-limited in unstirred syntheses.[4] Non-diffusion-limited growth implies that nutrient is present at all positions on the surface and growth is thus dependent solely on energetics of attachment. Such growth is characterized by the experimentally observed constant area terrace advance. Crucially, the computer model allows deposition at only one site on the surface per iteration. Though this might initially seem counter-intuitive, it prevents the influence of population distribution of site types, and thus leads to the correct growth patterns.

The final step in creating the model involved defining the relative growth times for the different site types. This process has profound impact on the ultimate nature of the growth observed. The growth times mirror intuitive site attachment energies, thus SURFACE sites have the longest growth time and U sites and SURROUND sites have the shortest growth time. To minimize the number of iterations required to see a reasonable degree of surface growth, these latter short growth times were chosen as one time unit. Other times have been optimized based upon the features observed in the experimental AFM images. The SURFACE site time was set at 1000 time units as this gave a reasonable degree of multiple nucleation. The EDGE site time dictates the speed at which a freshly nucleated site will commence growth. More importantly, the ratio of EDGE site/KINK site times dictates the overall shape of the terraces. If this ratio is too high then the terraces will tend to grow out in a circular fashion, since KINK site growth is the mechanism for blocking out terrace shape. The final ratio was chosen to be 30/2 time units. The evolution of growth produced by these times is illustrated in the fifteen frames of Figure 3. Frames 2–4, 7, and 14 highlight the

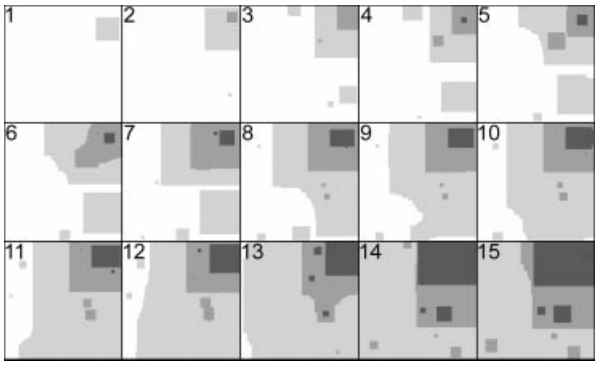

Figure 3. Fifteen frames that show the evolution of surface growth generated by the computer model. The frames are displayed in chronological order but were not necessarily taken at constant time intervals. Relative growth times, in arbitrary units, required to produce this simulation are, SURFACE 1000, EDGE 30, KINK 2, both U and SURROUND 1.

presence of multiple nucleation and the general square shape of the terraces. Frame 5 is taken shortly after the first terrace coalescence and highlights the formation of curved terrace edges. This phenomenon is repeated in further images though the curved terraces may be seen to grow out rapidly. The existence of convex terrace edges, as predicted by Monté Carlo growth simulation,[1b] is now confirmed in Figure 1. In terms of the most significant growth processes of surface nucleation, edge and kink growth the relative rates are:

$$500 \times \text{surface rate} = 15 \times \text{edge rate} = \text{kink rate}.$$

In conclusion, an accurate model of the surface growth of one of the most important industrial zeolites has been created. In conjunction with experimental data this model highlights the non-diffusion-limited nature of zeolite growth and furnishes the first rate data concerned with fundamental growth processes in zeolites.

Experimental Section

Atomic force micrographs were recorded on a Digital Instruments Nanoscope Multimode Microscope operating in TappingMode, recording height and phase information. The method used to prepare the samples for AFM and the synthesis procedure for the zeolite A crystals were reported in ref. [1b]. The computer simulation was written using the software package Mathematica 3.0 from Wolfram Research Inc. This package was chosen for ease of post-simulation image processing; however, future versions of the program will be coded in a high-level language.

Received: May 4, 2001 [Z17044]

[1] a) M. W. Anderson, J. R. Agger, J. T. Thornton, N. Forsyth, *Angew. Chem.* **1996**, *108*, 1301–1304; *Angew. Chem. Int. Ed. Engl.* **1996**, *35*, 1210–1213; b) J. R. Agger, N. Pervaiz, A. K. Cheetham, M. W. Anderson, *J. Am. Chem. Soc.* **1998**, *120*, 10754–10759; c) M. W. Anderson, J. R. Agger, N. Pervaiz, S. J. Weigel, A. K. Cheetham in *Proceedings of the 12th International Zeolite Conference*, *Vol. 3* (Eds.: M. M. J. Treacy, B. K. Marcus, M. E. Bisher, J. B. Higgins), Materials Research Society, Pennsylvania, **1998**, pp. 1487–1494; d) S. Sugiyama, S. Yamamoto, O. Matsuoka, T. Honda, H. Nozoye, S. Qiu, J. Yu, O. Terasaki, *Surf. Sci.* **1997**, *377*, 140–144.

[2] A. L. Weisenhorn, J. E. MacDougall, S. A. C. Gould, S. D. Cox, W. S. Wise, J. Massie, P. Maivald, V. B. Elings, G. D. Stucky, P. K. Hansma, *Science* **1990**, *247*, 1330–1333.

[3] a) J. E. MacDougall, S. D. Cox, G. D. Stucky, A. L. Weisenhorn, P. K. Hansma, W. S. Wise, *Zeolites* **1991**, *11*, 429–433; b) M. L. Occelli, S. A. C. Gould, G. D. Stucky, *Stud. Surf. Sci. Catal.* **1994**, *84*, 485–492; c) M. Komiyama, T. Yashima, *Jpn. J. Appl. Phys.* **1994**, *33*, 3761–3763; d) L. Scandella, N. Kruse, R. Prins, *Surf. Sci. Lett.* **1993**, *281*, 331–334; e) G. Binder, L. Scandella, A. Schumacher, N. Kruse, R. Prins, *Zeolites* **1996**, *16*, 2–6; f) S. Yamamoto, S. Sugiyama, O. Matsuoka, K. Kohmura, T. Honda, Y. Banno, H. Nozoye, *J. Phys. Chem.* **1996**, *100*, 18474–18482; g) S. Yamamoto, O. Matsuoka, S. Sugiyama, T. Honda, Y. Banno, H. Nozoye, *Chem. Phys. Lett.* **1996**, *260*, 208–214; h) W. H. Chen, H. C. Hu, T. Y. Lee, *Chem. Eng. Sci.* **1993**, *48*, 3683–3691.

[4] N. Hanif, M. W. Anderson, V. Alfredsson, O. Terasaki, *Phys. Chem. Chem. Phys.* **2000**, *2*, 3349–3357.

  1433-7851/01/4021-4067 $ 17.50+.50/0